

1 **Title:** Zinc²⁺ ion inhibits SARS-CoV-2 main protease and viral replication *in vitro*.

2 **Authors:** Love Panchariya^{1†}, Wajahat Ali Khan^{1†}, Shobhan Kuila^{1†}, Kirtishila Sonkar¹, Sibasis
3 Sahoo¹, Archita Ghoshal¹, Ankit Kumar², Dileep Kumar Verma², Abdul Hasan², Shubhashis
4 Das³, Jitendra K Thakur³, Rajkumar Halder⁴, Sujatha Sunil², Arulandu Arockiasamy^{1*}

5 **Affiliation:**

6 ¹Membrane Protein Biology Group, International Centre for Genetic Engineering and
7 Biotechnology, Aruna Asaf Ali Marg, New Delhi-110067. India.

8 ²Vector Borne Diseases Group, International Centre for Genetic Engineering and Biotechnology,
9 Aruna Asaf Ali Marg, New Delhi-110067. India.

10 ³Plant Mediator Lab, National Institute of Plant Genome Research, Aruna Asaf Ali Marg, New
11 Delhi- 110 067

12 ⁴Ruhvenile Biomedical OPC PVT LTD, Plot No-8, OCF Pocket Institution, Sarita Vihar, New
13 Delhi-110070. India.

14 [†]These authors contributed equally to the work presented.

15 For correspondence:

16 *Correspondence should be addressed to: sam@icgeb.res.in / asamy001@gmail.com

17 Communicating author:

18 Arockiasamy Arulandu

19 International Centre for Genetic Engineering and Biotechnology (ICGEB),

20 Aruna Asaf Ali Marg,

21 New Delhi 110067. India.

22 Phone: +91-11-26741358 Ext-172

23 Fax: +91-11-26742316

24 Mobile: +91-9711055502

25 **Abstract:**

26 Zinc deficiency is linked to poor prognosis in COVID-19 patients while clinical trials with Zinc
27 demonstrate better clinical outcome. The molecular target and mechanistic details of anti-
28 coronaviral (SARS-CoV2) activity of Zinc remain obscure. We show that ionic Zinc not only
29 inhibits SARS-CoV-2 main protease (Mpro) with nanomolar affinity, but also viral replication.
30 We present the first crystal structure of Mpro-Zinc²⁺ complex at 1.9 Å and provide the structural
31 basis of viral replication inhibition.

32

33 COVID-19 pandemic caused by SARS-CoV-2 is a major clinical challenge^{1,2,3}. Lower serum
34 Zinc concentration at the time of admission of COVID-19 patients correlates with severe clinical
35 presentations; an extended duration to recovery, higher morbidity, and a higher mortality in
36 elderly^{4,5}. However, clinical trials with Zinc and ionophore show positive clinical outcome with a
37 decreased rate of mortality, and transfer to hospice^{6,7,8}.

38

39 Zinc plays several key roles in biological systems viz. structural, catalytic, regulatory and
40 signalling events^{9,10,11}. Further, Zinc exhibits anti-viral properties¹², including anti-SARS-CoV.
41 SARS-CoV Main protease (Mpro)¹³ and RNA dependent RNA polymerase (RDRP)¹⁴ are
42 potential key molecular targets of Zinc. However, the structure of SARS-CoV-2 RDRP¹⁵
43 suggests a structural role for Zinc rather than an inhibitory one. Notably, detailed kinetics and
44 mechanism of ionic Zinc targeting SARS-CoV-2 Mpro is lacking.

45

46 We first studied one on one binding kinetics of Zinc acetate with purified SARS-CoV-2 Mpro
47 using Surface Plasmon Resonance (SPR). Zinc binds to SARS-CoV-2 Mpro with an association
48 rate constant (ka) of $8,930 \pm 30 \text{ M}^{-1} \text{ s}^{-1}$ and the dissociation rate constant (kd) of $0.01755 \pm 10 \text{ s}^{-1}$,
49 and an equilibrium dissociation constant (KD) of $1.965 \text{ E}^{-06} \text{ M}$. (**Fig. 1a**) The half-life ($t_{1/2} = \ln$
50 $[0.5]/kd$) of Zinc-Mpro complex is computed to be $\sim 10 \text{ s}$. We then assessed the inhibitory effects
51 of Zinc²⁺ binding on the proteolytic activity of SARS-COV-2 Mpro in the presence of Zinc
52 acetate. We obtained an IC₅₀ value of $325.1 \pm 5.1 \text{ nM}$ with complete inhibition at $6.25 \text{ } \mu\text{M}$ and

53 above (**Fig. 1b**). We also tested Zinc glycinate and Zinc gluconate complexes, which are
54 available as Zinc supplements in the market and are also investigated in COVID-19 clinical
55 trials¹⁶, and obtained IC₅₀ values of 279.35±17.95 nM and 405.25±0.45 nM, respectively
56 (**Supplementary Figure 1, a and b**). Reversibility of Zinc²⁺-mediated inhibition was tested by
57 first inhibiting the enzyme with 500 nM Zinc acetate, and then initiating the reaction with a
58 substrate peptide, followed by addition of EDTA to regain the enzyme activity by chelating
59 Zinc²⁺ ions. We find that Zinc inhibition is completely reversible by EDTA (**Supplementary**
60 **Figure 1, c**), suggesting that inhibition by the metal ion is not because of oxidation of catalytic
61 cysteine (Cys145).

62

63 To further understand the structural basis of SARS-CoV-2 Mpro inhibition by Zinc²⁺ ion, we
64 solved the crystal structure of Zinc²⁺ bound complex at 1.9 Å (**Supplementary Table 2**). The
65 asymmetric unit contains a dimer of Mpro in space group P2₁2₁2₁ (**Fig. 1c**). An unambiguous
66 electron density for Zinc²⁺ (**Fig. 1d, e**) shows that the metal ion is coordinated by the catalytic
67 dyad His41 and Cys145, which is absent in the control datasets collected for apo-enzyme crystals
68 grown in the same condition. Zinc²⁺-bound complex shows a tetrahedral coordination geometry
69 at the Mpro active site by coordinating with two water molecules that are absent in the apo-
70 enzyme structure (**Fig. 1c**). Distortion in the tetrahedral geometry observed is attributed to the
71 presence of heterogeneous atoms; sulphur (Cys145-SG) and nitrogen (His41-NE2) in the
72 inhibited complex. A 180° flip of the imidazole ring of His41 brings NE2 closer to Zinc²⁺ with
73 an inter-atomic distance of 1.94 Å to form a coordinate bond. The interatomic distance between
74 catalytic Cys145 and Zinc is 2.36 Å consistent with observed bound complexes. Two structural
75 water molecules W1 and W2 (PDB: 7DK1; HETATM 5028 and 5031, respectively) coordinate
76 Zinc²⁺ at an inter-atomic distance of 2.23 Å and 1.98 Å, respectively, to satisfy the tetrahedral
77 geometry (**Fig. 1c**). The coordination of Zinc²⁺ with the catalytic dyad is expected to prevent a
78 nucleophilic attack on the carbonyl moiety of the amide bond in polyprotein substrate. We
79 hypothesize that the two strongly coordinated water molecules impart stability to the Zinc²⁺
80 inhibited complex.

81

82 To gain deeper insights into the stability of Mpro- Zinc²⁺ complex, we simulated the complex for
83 1 μ s at 300K, keeping the coordinating waters, W1 and W2. During the simulation, Zinc²⁺
84 remains strongly bound to the active site via metal coordination bonds with His41 (NE2) and
85 Cys145 (SG) with an interatomic distance of 1.951 ± 0.031 and 2.518 ± 0.031 Å, respectively,
86 throughout the 1 μ s time frame. The mobility of Zinc²⁺ ion is restricted with a mean RMSD of
87 0.920 Å (**Fig. 1f**) in accordance with the dynamics of side chains of coordinating catalytic dyad.
88 Visualization of MD simulation trajectory shows (**Supplementary Movie**) that coordinating
89 water molecules W1 and W2 remain bound to Zinc²⁺ throughout the simulation, and help
90 maintain the tetrahedral geometry observed in complex crystal structure (**Fig. 1g**).

91
92 We further assessed the inhibitory potential of Zinc acetate, Zinc glycinate and Zinc gluconate
93 against SARS-COV-2. Infected Vero E6 cells were treated with all the three Zinc salts at their
94 respective maximum non-toxic concentrations (MNTD) for 48 hours. The MNTDs used for the
95 three compounds were 100 μ M for Zinc acetate and Zinc gluconate and 70 μ M for Zinc
96 glycinate. We observed that Zinc acetate treatment resulted in more than 50% reduction of viral
97 titre, as compared to the untreated infected cells (**Fig. 2a**). Based on these results, we determined
98 the IC₅₀ of Zinc acetate to be 3.227 μ M (**Fig 2b**). Surprisingly, Zinc glycinate and Zinc
99 gluconate failed to inhibit viral replication in standard antiviral assays at non-toxic
100 concentrations albeit showing effective enzyme inhibition *in vitro*. Quercetin, a natural Zinc
101 ionophore, increases the bioavailability of Zinc in treated cells¹⁷, which prompted us to ask
102 whether an increased bioavailability of Zinc²⁺ results in enhanced inhibition of viral replication.
103 To test this, we mixed Zinc acetate with Quercetin at 1:2 molar ratio¹⁸ at non-toxic
104 concentrations (**Supplementary Figure 2**) and tested the antiviral activity against SARS-CoV-2.
105 We observed >2-fold viral inhibition in the presence of Quercetin (**Fig. 2c**).

106
107 Taken together, our data strongly suggest an inhibitory role for ionic Zinc¹⁰, wherein it inhibits
108 SARS-CoV-2 Mpro enzyme activity, supported by complex crystal structure and subsequent
109 inhibition of viral replication *in vitro*. Known crystal structures of Zinc conjugates such as N-
110 ethyl-n-phenyl-dithiocarbamic acid (EPDTC), JMF1600, and Zinc-pyrithione in complex with
111 3C-like (Mpro) proteases from coronaviruses¹⁹, including SARS-CoV²⁰ and SARS-CoV-2²¹,

112 show a similar mode of metal ion coordination with the catalytic dyad (**Supplementary Figure**
113 **3**). However, the Zinc²⁺ inhibited SARS-CoV-2 Mpro enzyme structure presented in this study
114 clearly suggests that ionic form of Zinc alone is capable of inhibiting the enzyme, by forming a
115 stable complex at the active site with the help of two water molecules, previously unknown. We
116 further show Zinc complexes; Zinc glycinate and Zinc gluconate failed to produce any antiviral
117 effects in our cell culture experiments, in agreement with a recent clinical trial data¹⁶ that show
118 no significant effect of Zinc gluconate in clinical outcome in COVID-19 patients. Most notably,
119 we show that Zinc ionophore Quercetin aids in inhibition of SARS-CoV-2 replication as it
120 increases the intracellular concentration of Zinc¹⁷. Our data support the findings that a
121 combination of Zinc salt, which provides ionic Zinc, with ionophores⁶⁻⁸, may have a better
122 clinical outcome in COVID-19 therapy. As the Zinc²⁺ coordinating catalytic dyad; Cysteine and
123 Histidine, is present across all coronaviral 3C-like protease (Mpro) active sites, including the
124 ones coded by virulent strains of SARS-CoV-2, the mode of Zinc²⁺ inhibition is expected to be
125 conserved. Short half-life (~10s) of Mpro-Zinc²⁺ complex, fast association and dissociation rates,
126 and water-soluble nature of Zinc acetate suggest that constant doses of Zinc-ionophore
127 combination may be required for effective inhibition of SARS-CoV-2 Mpro.

128

129 **Data accessibility:** Mpro-Zinc²⁺ complex coordinates are available at PDB: 7DK1. X-ray raw
130 data is available from Integrated Resource for Reproducibility in Macromolecular
131 Crystallography (IRRM) repository (<https://proteindiffraction.org/>).

132

133 **Acknowledgement:** We thank Prof. Rolf Hilgenfeld, Institute of Biochemistry, University of
134 Lübeck, Lübeck, Germany for providing the expression construct for SARS-CoV-2 Mpro. We
135 thank the beamline staff at the Elettra XRD2 particularly Raghurama P. Hegde and Annie
136 Heroux for beamline support. Access to the XRD2 beamline at the Elettra synchrotron, Trieste
137 was made possible through grant-in-aid from the Department of Science and Technology, India,
138 vide grant number DSTO-1668. The following reagent was deposited by the Centers for Disease
139 Control and Prevention and obtained through BEI Resources, NIAID, NIH: SARS-Related
140 Coronavirus 2, Isolate USA-WA1/2020, NR-52281. We thank Prof. Ramesh Sonti, former

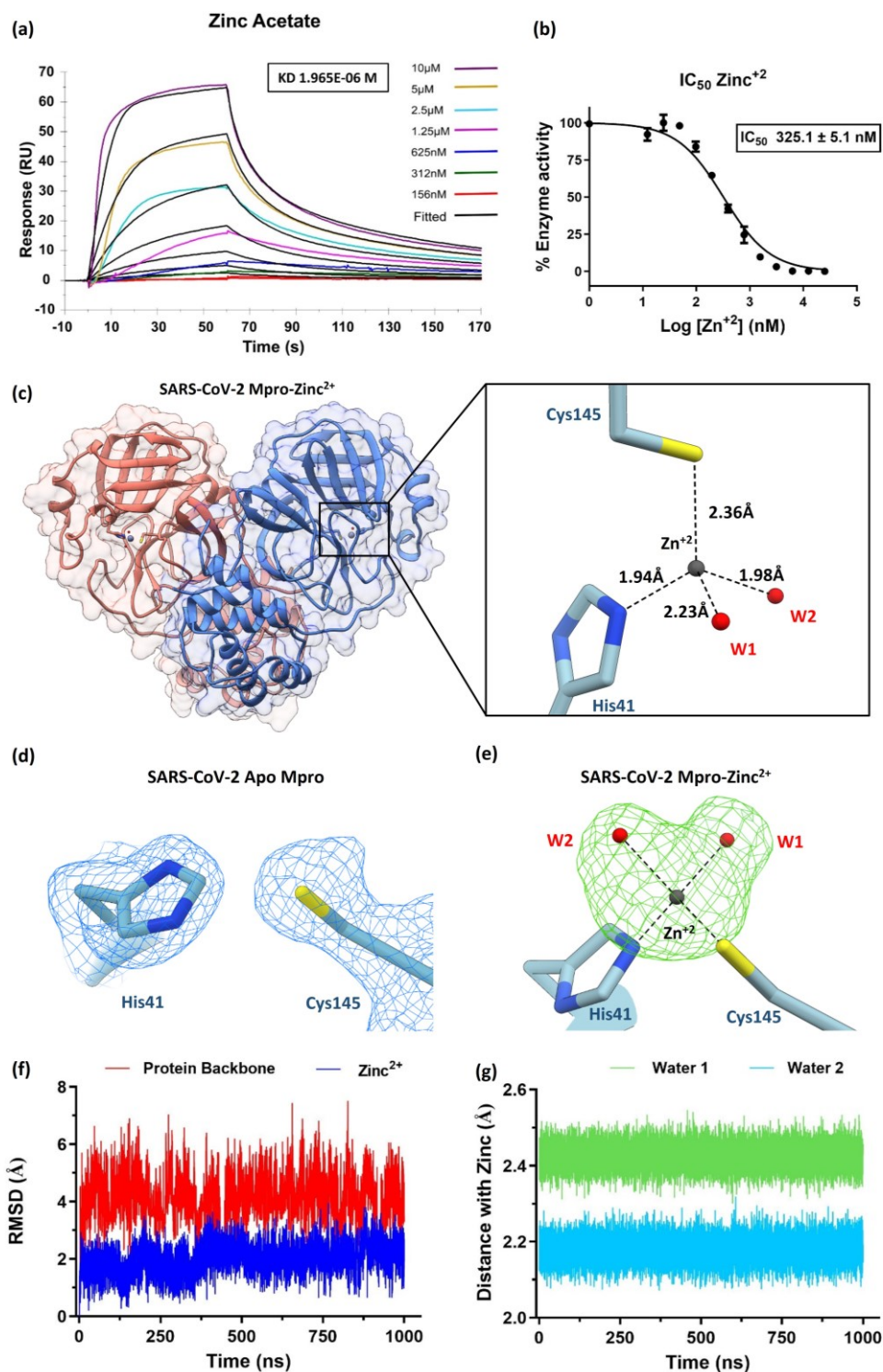
141 Director, NIPGR, New Delhi for access to Biacore T-200. This work was supported by ICGEB
142 core grant and Govt. of India DST-SERB IRHPA grant: IPA/2020/000285 to AA and S. Sunil.

143

144 **Author contribution:** LP, WK, SK, KS purified Mpro and performed biochemical and SPR
145 experiments and SD and JKT helped with SPR experiments and data analysis. LP and KS
146 crystallized, collected X-ray data and solved the structure. LP and SS performed MD simulation
147 and analysis. AG performed cytotoxicity assays. AK, DV, AH and S. Sunil performed anti-viral
148 assays and analysed the data. RH provided inputs to biochemical assays. AA coordinated the
149 work and LP and AA wrote the manuscript with inputs from all the authors.

150 **Conflict of interest:** The authors declare no conflict of interest.

151



152

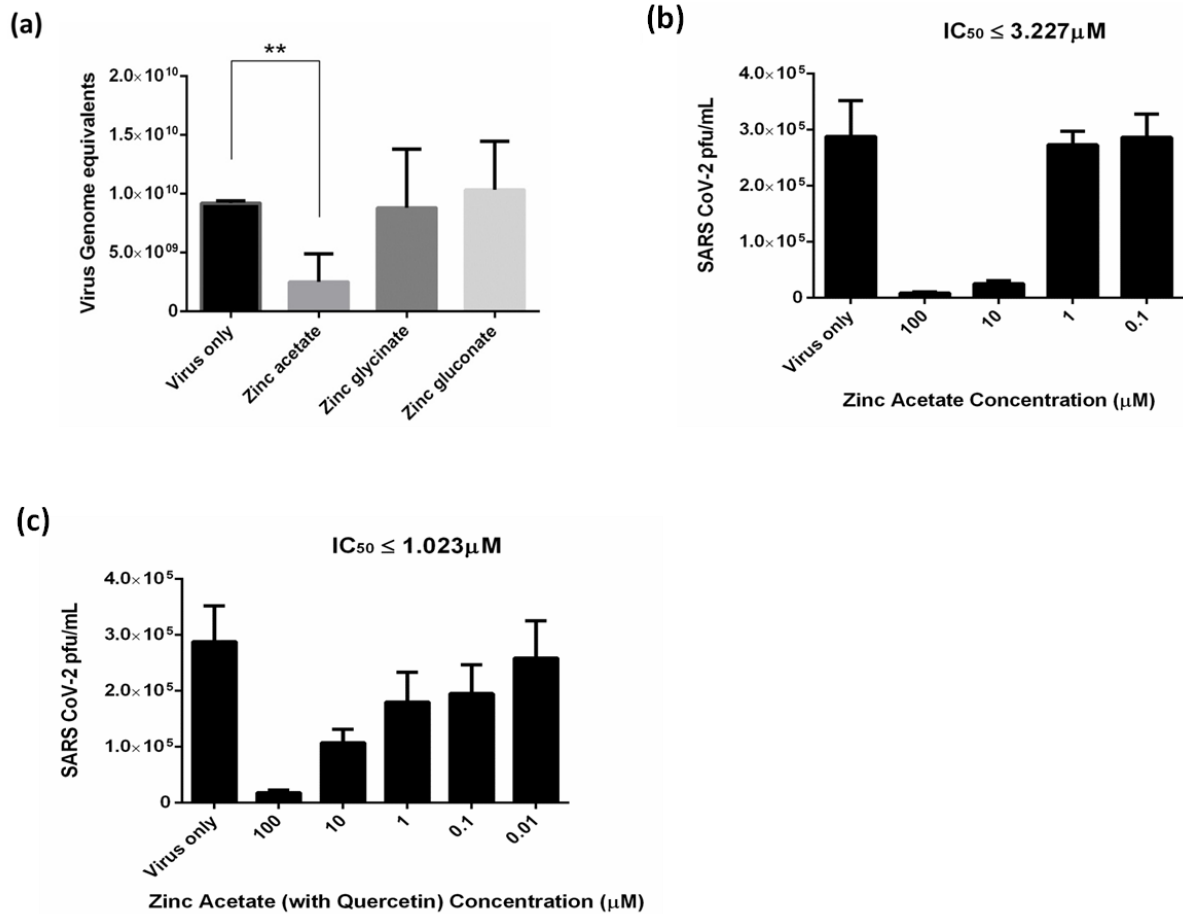
153 **Figure 1. Zinc $^{2+}$ binds at the active site and inhibits SARS-CoV-2 Mpro enzyme activity:**

154 **(a)** Interaction kinetics of Zinc $^{2+}$ with immobilized Mpro using surface plasmon resonance (SPR)

155 shows affinity (KD) of 1.96 μ M. Coloured lines indicate various concentrations of Zinc acetate.

156 **(b)** IC₅₀ and concentration dependent inhibition of Mpro by Zinc²⁺ ion. **(c)** Complex crystals
157 structure of Mpro dimer with Zinc (grey sphere) bound at the active site of both protomers. On
158 the right, catalytic dyad Cys145 and His41 of Mpro is shown with bound Zinc in tetrahedral
159 coordination geometry. **(d)** Electron density map (2Fo-Fc) contoured at 1 σ showing the catalytic
160 dyad in Apo-Mpro **(e)** Omit difference map (Fo-Fc contoured at 3 σ) shows unambiguous
161 density (green) for Zinc²⁺ (grey) and two metal-ion coordinating structural water molecules
162 (red). **(f)** 1 μ s MD simulation Mpro-Zinc²⁺ complex shows low RMSD of Zinc²⁺ (blue) and
163 protein backbone (red) indicating stability of inhibited state **(Supplementary video)** **(g)** Distance
164 plot shows less fluctuations in inter-atomic distances between Zinc²⁺ and two coordinating water
165 molecules during the course of simulation, representing stable metal ion-water interactions in the
166 inhibitory role of Zinc²⁺.

167



168

169 **Figure 2. Anti-SARS-CoV-2 activity of Zinc and its complexes with ionophore in infected**
170 **Vero E6 cells. a)** Zinc acetate inhibits SARS-CoV-2 replication in Vero E6 cells as determined
171 using qRT-PCR. Treatment with Zinc acetate (100 μM) for 48 h resulted in >50% reduction of
172 viral titre while the Zinc glycinate and Zinc gluconate complexes did not show significant
173 reduction. **(b)** IC₅₀ determination using varying concentrations of Zinc for 48 h followed by viral
174 quantification using plaque assay. **(c)** Viral inhibition by Zinc acetate and Quercetin mixture (1:2
175 M ratio). Mean percentage reduction of SARS-CoV-2 is indicated within the bars. The antiviral
176 experiments were repeated at least twice, and each experiment included at least three replicates.
177 Statistical significance was determined using Student's t-test (n ≥ 2 biological replicates).

178

179

180

181 **References**

- 182 1 Wu, F. *et al.* A new coronavirus associated with human respiratory disease in China. *Nature* **579**,
183 265-269, doi:10.1038/s41586-020-2008-3
- 184 10.1038/s41586-020-2008-3 [pii] (2020).
- 185 2 Wise, J. Covid-19: New coronavirus variant is identified in UK. *BMJ* **371**, m4857,
186 doi:10.1136/bmj.m4857 (2020).
- 187 3 Yadav, P. D. *et al.* Isolation and characterization of the new SARS-CoV-2 variant in travellers from
188 the United Kingdom to India: VUI-202012/01 of the B.1.1.7 lineage. *J Travel Med* **28**, doi:taab009
189 [pii]
- 190 10.1093/jtm/taab009
- 191 6121695 [pii] (2021).
- 192 4 Jothimani, D. *et al.* COVID-19: Poor outcomes in patients with zinc deficiency. *Int J Infect Dis* **100**,
193 343-349, doi:S1201-9712(20)30730-X [pii]
- 194 10.1016/j.ijid.2020.09.014 (2020).
- 195 5 Vogel-Gonzalez, M. *et al.* Low Zinc Levels at Admission Associates with Poor Clinical Outcomes in
196 SARS-CoV-2 Infection. *Nutrients* **13**, doi:562 [pii]
- 197 10.3390/nu13020562
- 198 nu13020562 [pii] (2021).
- 199 6 Carlucci, P. M. *et al.* Zinc sulfate in combination with a zinc ionophore may improve outcomes in
200 hospitalized COVID-19 patients. *J Med Microbiol* **69**, 1228-1234, doi:10.1099/jmm.0.001250
201 (2020).
- 202 7 Frontera, J. A. *et al.* Treatment with Zinc is Associated with Reduced In-Hospital Mortality
203 Among COVID-19 Patients: A Multi-Center Cohort Study. *Res Sq*, doi:rs.3.rs-94509 [pii]
- 204 10.21203/rs.3.rs-94509/v1 (2020).
- 205 8 Derwand, R., Scholz, M. & Zelenko, V. COVID-19 outpatients: early risk-stratified treatment with
206 zinc plus low-dose hydroxychloroquine and azithromycin: a retrospective case series study. *Int J*
207 *Antimicrob Agents* **56**, 106214, doi:S0924-8579(20)30425-8 [pii]
- 208 10.1016/j.ijantimicag.2020.106214 (2020).
- 209 9 Kochanczyk, T., Drozd, A. & Krezel, A. Relationship between the architecture of zinc coordination
210 and zinc binding affinity in proteins--insights into zinc regulation. *Metallomics* **7**, 244-257,
211 doi:10.1039/c4mt00094c (2015).
- 212 10 Maret, W. Zinc coordination environments in proteins determine zinc functions. *J Trace Elem*
213 *Med Biol* **19**, 7-12, doi:S0946-672X(05)00012-X [pii]
- 214 10.1016/j.jtemb.2005.02.003 (2005).
- 215 11 Maret, W. Inhibitory zinc sites in enzymes. *Biometals* **26**, 197-204, doi:10.1007/s10534-013-
216 9613-7 (2013).
- 217 12 Read, S. A., Obeid, S., Ahlenstiel, C. & Ahlenstiel, G. The Role of Zinc in Antiviral Immunity. *Adv*
218 *Nutr* **10**, 696-710, doi:10.1093/advances/nmz013
- 219 5476413 [pii] (2019).
- 220 13 Hsu, J. T. *et al.* Evaluation of metal-conjugated compounds as inhibitors of 3CL protease of SARS-
221 CoV. *FEBS Lett* **574**, 116-120, doi:10.1016/j.febslet.2004.08.015

- 222 S0014579304010087 [pii] (2004).
223 14 te Velthuis, A. J. *et al.* Zn(2+) inhibits coronavirus and arterivirus RNA polymerase activity in vitro
224 and zinc ionophores block the replication of these viruses in cell culture. *PLoS Pathog* **6**,
225 e1001176, doi:10.1371/journal.ppat.1001176 (2010).
226 15 Kokic, G. *et al.* Mechanism of SARS-CoV-2 polymerase stalling by remdesivir. *Nat Commun* **12**,
227 279, doi:10.1038/s41467-020-20542-0
228 10.1038/s41467-020-20542-0 [pii] (2021).
229 16 Thomas, S. *et al.* Effect of High-Dose Zinc and Ascorbic Acid Supplementation vs Usual Care on
230 Symptom Length and Reduction Among Ambulatory Patients With SARS-CoV-2 Infection: The
231 COVID A to Z Randomized Clinical Trial. *JAMA Network Open* **4**, e210369-e210369,
232 doi:10.1001/jamanetworkopen.2021.0369 (2021).
233 17 Dabbagh-Bazarbachi, H. *et al.* Zinc ionophore activity of quercetin and epigallocatechin-gallate:
234 from Hepa 1-6 cells to a liposome model. *J Agric Food Chem* **62**, 8085-8093,
235 doi:10.1021/jf5014633 (2014).
236 18 Bratu, M. *et al.* Biological Activities of Zn(II) and Cu(II) Complexes with Quercetin and Rutin:
237 Antioxidant Properties and UV-Protection Capacity. *Revista de Chimie* **65**, 544-549 (2014).
238 19 Lee, C. C. *et al.* Structural basis of inhibition specificities of 3C and 3C-like proteases by zinc-
239 coordinating and peptidomimetic compounds. *J Biol Chem* **284**, 7646-7655,
240 doi:10.1074/jbc.M807947200
241 S0021-9258(20)32476-5 [pii] (2009).
242 20 Lee, C. C. *et al.* Structural basis of mercury- and zinc-conjugated complexes as SARS-CoV 3C-like
243 protease inhibitors. *FEBS Lett* **581**, 5454-5458, doi:S0014-5793(07)01116-7 [pii]
244 10.1016/j.febslet.2007.10.048 (2007).
245 21 Gunther, S. *et al.* X-ray screening identifies active site and allosteric inhibitors of SARS-CoV-2
246 main protease. *Science* **372**, 642-646, doi:10.1126/science.abf7945
247 science.abf7945 [pii] (2021).
248
249
250